JOURNAL OF GEOPHYSICAL RESEARCH, VOL. 92, NO. A9, PAGES 10,111–10,117, SEPTEMBER 1, 1987

Magnetotails at Unmagnetized Bodies: Comparison of Comet Giacobini-Zinner and Venus

D. J. McComas and J. T. Gosling

Los Alamos National Laboratory, Los Alamos, New Mexico

C. T. Russell

Department of Earth and Space Sciences, University of California, Los Angeles

J. A. Slavin

Jet Propulsion Laboratory, Pasadena, California

Both Comet Giacobini-Zinner (G-Z) and Venus have magnetotails consisting of draped interplanetary magnetic field lines. This field line draping is caused by a velocity shear between regions of greater flow speeds away from the bodies and lesser flow speeds near to the bodies. Data obtained within the Venus magnetotail by the Pioneer Venus Orbiter and within the G-Z tail by the International Cometary Explorer traversal of G-Z have previously been combined with stress balance considerations to infer many of the physical characteristics of these two magnetotails. In the present paper we compare and contrast these physical characteristics and thereby examine those aspects of the interactions with the solar wind and draped magnetotail forming processes which are common at the two bodies, and those which are different. We find that the near ionopause environs play a crucial role in the tail formation process at both Venus and G-Z and that draping at the two very different sized bodies occurs on ionopause scale sizes. On the other hand, ion densities, downtail mass fluxes, tailward $\mathbf{J} \times \mathbf{B}$ forces, and lobe betas are factors of $\sim 10^4$, 50, 100, and 20 times greater in the G-Z tail than in Venus', while bulk flow speeds and ion temperatures are factors of ~ 15 and 240 times lower. These large quantitative differences in the properties within the two magnetotails are attributable to the significantly greater upstream mass loading of the solar wind by the extended neutral atmosphere at G-Z (comets in general) compared to the gravitationally bound atmosphere of Venus.

1. Introduction

Magnetotails arise out of the solar wind's interaction with the magnetic fields and atmospheres of planetary and cometary bodies throughout the solar system. While the details of magnetotail structures vary from one body to the next, certain attributes are inherent to magnetotails in general. These include the juxtaposition of two lobes of nearly oppositely directed magnetic fields and a field reversing current sheet which acts to separate them. Through these cross tail current sheets the magnetic field rotates from one lobe's orientation to the other, everywhere self-consistently satisfying Ampere's Law.

The nature of the interaction between the solar wind and a planetary-cometary body depends fundamentally on the characteristics of the obstacle presented by that body to the solar wind. The solar wind flow and imbedded interplanetary magnetic field (IMF) are essentially excluded from various solar system obstacles by either an intrinsic planetary magnetic field or by a conductive ionosphere. At bodies with substantial intrinsic magnetic fields, such as Earth, Mercury, Jupiter, Saturn, and Uranus, the solar wind flow is nearly entirely diverted around the region dominated by this intrinsic field.

At bodies which lack substantial intrinsic magnetic field, but possess appreciable gaseous atmosphere, such as comets, Venus, and possibly some of the outer solar system planetary satellites such at Titan, the solar wind flow is slowed by mass loading and pressure gradients which build up due to exclusion of the flow by a conductive ionosphere. In contrast to the magnetotails of bodies with substantial intrinsic fields, magnetotails as these bodies are comprised of magnetic flux of purely solar origin. The plasma in such a magnetotail, on the other hand, is a mixture of solar wind and heavy ions of planetary or cometary origin. This planetary-cometary material is added to the flow when it becomes ionized by processes such as photoionization and charge exchange. In this study we refer to such magnetotails as "accreted" magnetotails in order to differentiate them clearly from magnetotails at bodies with substantial intrinsic magnetic fields.

An accreted magnetotail forms because of slowing of the plasma flow along streamlines which pass close to an obstacle. This slowing causes draping of the imbedded magnetic field about that obstacle in a manner first suggested by *Alfvén* [1957]. Slowing of the flowing solar wind near to an obstacle occurs because of (1) mass loading [*Harwit and Hoyle*, 1962; *Biermann et al.*, 1967] and (2) pressure gradients associated with exclusion of the magnetized plasma by an electrically conducting ionosphere [e.g., *Spreiter and Stahara*, 1980] which may additionally viscously interact [*Perez-de-Tejada*, 1982] with it. In solar system applications these two effects often work in concert to form draped magnetotails, and it is difficult to ascertain a priori their separate importances for the tail formation process. In particular, both effects seem to play important roles at both G-Z and Venus and together additionally interact to enhance tail formation as we discuss in section 5.2.

Paper number 7A8980.
0148-0227/87/007A-8980$02.00

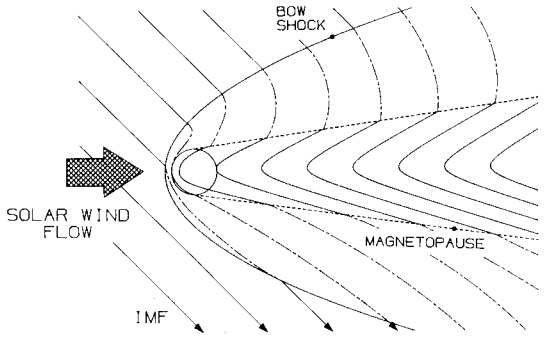

Fig. 1. Schematic diagram of magnetic field draping at an unmagnetized but conductive and mass loading obstacle (Venus, in this case) projected into a plane containing the upstream magnetic field and solar wind flow vectors and passing approximately through the center of the obstacle. A velocity shear between flows along stream lines which pass closer (slower flow) and further (faster flow) from the obstacle causes the imbedded magnetic field to drape into a magnetotail configuration with nearly oppositely directed tail lobes and a field reversing cross tail current sheet.

The resultant field topology of such magnetic field draping about Venus is shown schematically [from *McComas et al.*, 1986*a*] in Figure 1. The magnetic field lines shown here are projected into a plane defined by the upstream plasma flow and magnetic field vectors and passing through the central portion of the planet. The magnetic field in the sheath (between the bow shock and magnetopause) continues to be carried along by the relatively unimpeded flow while the flow passing nearest to the obstacle is most highly slowed. Since the field links the regions of greater and lesser flow speeds, the field becomes draped into a magnetotail configuration, complete with oppositely directed tail lobes and a central field reversing current sheet. The upstream flow is diverted around the obstacle and the flow perpendicular to the plane of this draping (into and out of the plane of the figure) carries the field over and under the obstacle and ultimately into the tail current sheet region [e.g., *Saunders and Russell*, 1986, Figure 20].

2. Venus and Comet Giacobini-Zinner

Venus and Comet Giacobini-Zinner provide the only examples of magnetotails at unmagnetized bodies in the solar system for which actual in situ observations are available. In this study therefore we limit our comparison of accreted magnetotails to these two. Inferences drawn from this comparison should not be considered to be overly general; on the other hand, at present, these magnetotails are the only ones where the tail formation process at unmagnetized bodies can be examined directly.

By far the greatest amount of data on the Venus magnetotail has been provided by the Pioneer Venus Orbiter (PVO) which has been in orbit about Venus since 1978. Although the Venus magnetotail exhibits a tremendous amount of temporal variability, the average magnetic configuration of the Venus magnetotail has been studied statistically [*Russell et al.*, 1981; *Slavin et al.*, 1984; *Marubashi et al.*, 1985; *Saunders and Russell*, 1986; *McComas et al.*, 1986*a*]. The PVO plasma instruments were designed primarily for making measurements either in the ionosphere or the solar wind and are generally unable to resolve ions in the deep Venus magnetotail [*Slavin et al.*, 1984; *McComas et al.*, 1986*b*]. However, these instruments have observed ionized atomic oxygen being picked up by the sheath flow [*Mihalov and Barnes*, 1981] as well as "clouds" of ionospheric plasma apparently being pulled off the ionosphere at lower altitudes [*Brace et al.*, 1982]. Since these instruments do not provide direct measurements of the average plasma properties in the Venus magnetotail, in the present study parameters given for these average properties will be taken from the work by *McComas et al.* [1986*a*] which used MHD stress balance conditions to derive the self-consistent, average plasma properties of the Venus tail from the average field configuration.

The magnetotail traversal of Comet Giacobini-Zinner by the International Cometary Explorer (ICE) on September 11, 1985, represents the first and, at present, the only in situ observations of a cometary magnetotail. Unlike the PVO data set discussed above, the G-Z magnetotail data set consists of both plasma electron measurements [*Bame et al.*, 1986; *Meyer-Vernet et al.*, 1986] and magnetic field measurements [*Smith et al.*, 1986]. The field data for the 8 min around closest approach (1059:40–1107:40) exhibit clear evidence for a magnetotail type structure including roughly antiparallel pointing magnetic lobes separated by a field rotating magnetotail current sheet [*Smith et al.*, 1986; *Slavin et al.*, 1986*a*, *b*; *Slavin et al.*, 1987]. While the plasma density generally increases with decreasing distance from the cometary nucleus [*Bame et al.*, 1986; *Zwickl et al.*, 1986], the current sheet region is observed to contain an additional very dense (>600 cm^{-3}) and cold ($\sim 10^4$ K) plasma sheet plasma.

Since the ICE data set consists of only a single 8-min tail crossing, no statistical derivation of the average tail properties is possible. On the other hand, both magnetic field and plasma observations are available for the ICE tail crossing, unlike with PVO. Taken together, these combined data sets allow for a much more complete analysis of the single ICE tail crossing than is possible for single orbits at Venus. From an MHD stress balance analysis of the combined plasma and magnetic field data, the unmeasured ion properties at ICE and the upstream conditions at the average pick up locations near to the comet nucleus have been derived [*Siscoe et al.*, 1986; *McComas et al.*, 1987]. In the present study, parameters given for the Comet Giacobini-Zinner magnetotail fields and plasma properties will be taken from *McComas et al.* [1987] unless otherwise referenced.

While many aspects of the solar wind–IMF interaction with G-Z and Venus are similar, a number of differences also exist. These differences affect tail formation at the two bodies, leading to major quantitative differences between the properties in the two magnetotails. The primary difference between the obstacles presented to the solar wind–IMF by these two bodies is related to the gravitational binding of their respective neutral atmospheres. At comets the solid nucleus is small ($\sim$km in diameter) and nonmassive ($\sim 10^{12}$-10^{18} kg) so that neutral atoms and molecules liberated from the nucleus surface are not gravitationally bound. Rather, material sublimed from the surface flows outward from the nucleus with a characteristic speed of ~ 1 km/s (for H_2O). Effects of this neutral outflow from G-Z have been observed at distances at least as great as 2.7×10^6 km [*Scarf et al.*, 1986], and the solar wind bulk flow speed was measurably slowed due to the pick up of cometary ions at distances of $\sim 1.5 \times 10^5$ km from the nucleus, along the ICE trajectory [*Bame et al.*, 1986].

Compared to solid cometary nuclei, Venus is much larger ($\sim$6100 km radius) and more massive ($\sim 4.87 \times 10^{24}$ kg). The

escape velocity from Venus is ~ 10.3 km s^{-1}, so that the neutral atmosphere is tightly bound to the planet. Thus the amount of neutral gas above the Venus ionosphere is limited and drops off very quickly with distance from the planet. Planetary ion pick up is therefore negligible far from the ionosphere, and the plasma flow directly upstream from the planet is slowed only over the relatively short distance behind the shock. Thus while Venus is $\sim 10^3$ times larger than solid cometary nuclei, the actual region of interaction with the solar wind is $\sim 10^2$ times smaller.

Other, more subtle, factors also play roles in defining the exact properties and structures of the magnetotails formed at these two bodies. These include the atmospheric chemistry and composition, rotation rates, and at least at comets, the surface properties such as fissuring and gas-dust jets. In general, these factors probably produce effects which are too subtle to be resolved uniquely in the two body comparison undertaken in this study, and we will concentrate on effects caused by the differing atmospheric-ionospheric configurations.

3. Scale Sizes

In Figure 2 the characteristic scale sizes for the solar wind interactions and magnetotails at Giacobini-Zinner (top) and Venus (bottom) are compared. Both halves are scaled by the appropriate ionopause radii R_{ip} for the two bodies. Ionopause radii provide a natural common ground for the comparison of these magnetotails if draping of the IMF about the ionospheric obstacle is primarily responsible for the observed magnetotail configurations. In this study we demonstrate that draping does occur on the ionopause scale size and vindicate the use of R_{ip} for comparing the G-Z and Venus magnetotails. For R_{ip} at Venus we use Venus radii ($R_V \sim 6100$ km), since the quantities of interest have already been calculated in R_V by *McComas et al.* [1986*a*] and the two radii are equal to within a few percent (better than the errors inherent in the calculations of these properties). For comets the ionopause radius can be derived by equating the neutral drag and electromagnetic body forces acting on a parcel of plasma at the ionopause [*Ip and Axford*, 1982]. For the solar wind and cometary conditions at the time of the ICE encounter with G-Z, this value is approximately 600 km [*Mendis et al.*, 1986].

Note that the G-Z bow wave in Figure 2 is drawn at a subsolar position of ~ 70 R_{ip} upstream from the nucleus, while the Venus bow shock stands off only ~ 0.3 R_{ip} above the planetary ionosphere. This indicates that whereas the Venus magnetotail is a large component of the overall planetary interaction with the solar wind, the cometary magnetotail is only a very small structure imbedded within a much greater region of cometary mass loading and interaction. In this study, only this small magnetotail structure will be examined in detail.

In order to make a valid comparison of the Venus and Comet Giacobini-Zinner magnetotails, it is first necessary to ascertain that equivalent portions of the two tails have been sampled and analyzed by the PVO and ICE spacecraft. ICE traversed G-Z $\sim 7.8 \times 10^3$ km antisunward from the cometary nucleus. PVO, on the other hand, is in a highly elliptical orbit about Venus, which has an apoapsis of $\sim 7 \times 10^4$ km. Since the spacecraft is moving most slowly near apoapsis, the majority of the data are taken near this distance, and the range of downtail distances of the PVO tail data is -4.8×10^4 to -7.3×10^4 km [e.g., *McComas et al.*, 1986*a*].

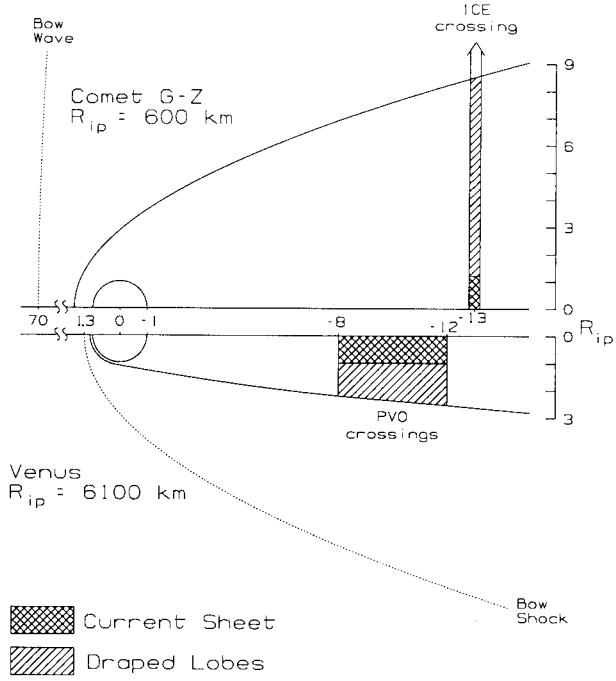

Fig. 2. Comparison of the important scale sizes of the (top) G-Z and (bottom) Venus interactions with the solar wind in the planes containing the upstream solar wind velocity and IMF vectors and passing through the centers of the obstacles. All sizes are normalized to the appropriate units for magnetic field draping: ionopause radii, R_{ip}. G-Z tail is a very small structure imbedded in a much larger region of mass loading, characterized by the bow wave at ~ 70 R_{ip}, whereas the Venus tail constitutes a large fraction of the solar wind interaction region. Note that the current sheets in both tails have thicknesses very nearly equal to the ionopause obstacle diameter indicating the importance of the ionopauses in current sheet and therefore tail formation.

At first glance the observations at G-Z and Venus seem incompatible due to the fact that the Venus magnetotail measurements were taken nearly 10 times further downtail than were the G-Z measurements. The ionospheric obstacle at Venus, however, is also ~ 10 times greater than at G-Z so that the size scale of the entire magnetotail is expected to be proportionally larger at Venus. As is indicated in Figure 2, the regions studied at downtail distances of -8 to -12 (Venus) and ~ -13 (G-Z) ionopause radii are quite similar. This similarity provides substantial justification for the direct comparison of the ICE and PVO data used in this study.

Magnetotail diameters at these comparable distances are of the same order. While the Venus tail diameter is ~ 3 times greater than the G-Z tail diameter (3.1×10^4 versus 1.0×10^4 km), it is ~ 3 times smaller in the appropriate scaling units of ionopause radii. The final scale sizes to note in Figure 2 are the thicknesses of the current sheets in the G-Z and Venus magnetotails. Both current sheets are approximately two ionopause radii thick, or in other words, about the diameter of the ionospheric obstacle upstream.

4. Comparison of Magnetotail Properties

Average magnetic field vectors as a function of location across the Venus magnetotail are displayed in the left panel of Figure 3. This plot is drawn in the X-Y^* plane of a Venus centered coordinate system where the planet is at the top of the page, and the Y^* axis is statistically constructed to point

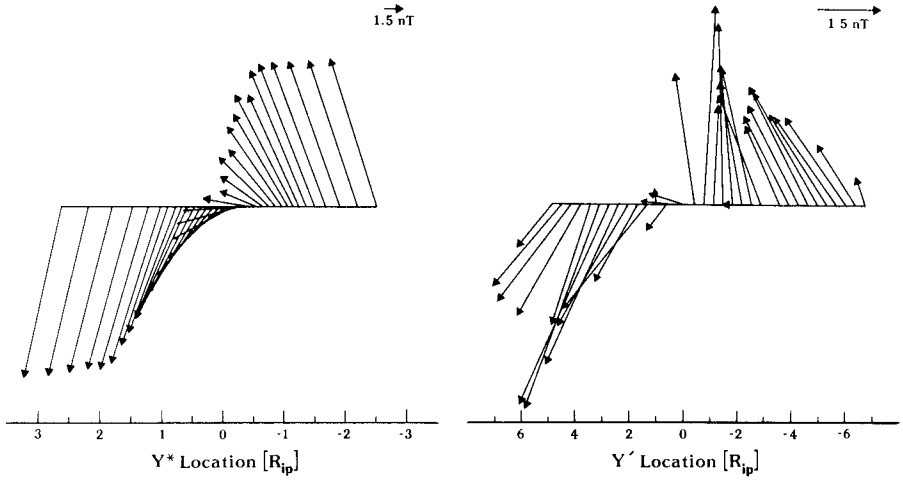

Fig. 3. Comparison of the magnetic field draping patterns across the (left) Venus and (right) Comet Giacobini-Zinner magnetotails. Draping pattern shown for Venus is a statistical result based on ~10,000 one-minute-averaged data samples, whereas the G-Z draping was measured for only the single ICE tail traversal; thus temporal variations are averaged out in the Venus case but are present in the G-Z data. Still, the overall magnetic field draping in these two magnetotails is qualitatively quite similar (see text for details).

in the direction of the average cross tail component of the magnetic field [*McComas et al.*, 1986*a*]. The rotation of the field across the tail is quite smooth since the variation displayed in this panel was built up out of a very large statistical data set (~10^4 one-minute-averaged field vectors) and variations due to time dependent effects have been averaged out. Note that the rotation of the field through the current sheet occurs over approximately two Venus radii as indicated in the previous discussion.

The right-hand panel of Figure 3 [from *Slavin et al.*, 1986*a*] displays the magnetic field draping pattern across the Giacobini-Zinner magnetotail in the plane defined by the solar direction and normal to the ecliptic plane, and passing through the center of the comet. The sun is toward the top of the panel. In order to make the two panels more directly comparable the cross tail location across the bottom has been labeled in ionopause radii perpendicular to the cross tail current sheet (Y'). The current sheet is inclined ~45° with respect to the ecliptic plane [*Slavin et al.*, 1987] so that the apparent thickness of this regon is greater along the ICE trajectory than along the Y' axis. In addition, this current sheet orientation combined with the slightly off-center trajectory of ICE through the tail causes the apparent difference in the thicknesses of the two tail lobes [*McComas et al.*, 1987]. Unlike the large statistical data set available for Venus, the field vectors in the right-hand panel represent 15-s averaged measurements taken along the single ICE fly through of the cometary magnetotail.

Even though the two magnetic field draping patterns displayed in Figure 3 are not taken in exactly equivalent planes, the overall variations displayed are qualitatively similar. Both panels show draped magnetotail configurations with two essentially oppositely directed lobes separated by cross tail current sheets. The characteristic lobe field strengths in the two tails are of the same order, with the G-Z lobe field strength being a factor of 2–5 times the ~13 nT value at Venus. Furthermore, the G-Z lobe field exhibits a factor of 2 increase in magnitude in going from the magnetopause into the lobe region adjacent to the plasma sheet [*Slavin et al.*, 1986*a*; *Slavin et al.*, 1987].

The quantitative electromagnetic properties derived from the measured field variations and averaged across the two current sheets are displayed in the top two rows of Table 1. The current densities displayed in the table have been calculated from the curl of the measured magnetic fields according to Ampere's Law. For Venus, both components of the curl (dB_X/dY^* and dB_{Y^*}/dX) were available from the statistical data set and were used to derive the value of ~1.4 nA m^{-2}. While both of the terms in the curl were used at Venus, the DB_{Y^*}/dX term constituted less than 10% of the total current density in the current sheet. At G-Z, the dB_X/dZ term and knowledge of the angle of inclination of the current sheet normal Y' were combined to calculate the typical current

TABLE 1. Quantitative Comparison of the Approximate Properties in the Venus and Giacobini-Zinner Magnetotails

	Venus[a] (O^+)	Comet G-Z[b] (H_2O^+)	Units
Current density			
Current sheet	1.4	100	nA m^{-2}
$(\mathbf{J} \times \mathbf{B})_X$ force			
Current sheet	-1×10^{-17}	-1×10^{-15}	N m^{-3}
Flow speed	−370[c]	−25[c]	km s^{-1}
Acceleration			
Current sheet	−6200[d]	−55[d]	m s^{-2}
Plasma density			
Current sheet	0.06	600	cm^{-3}
Lobes	0.005	100	cm^{-3}
Ion temperature			
Current sheet	$<9 \times 10^7$	1×10^5	Kelvin
Lobes	$>9 \times 10^7$	$0.3 - 1 \times 10^6$	Kelvin
Beta			
Lobe	0.1	2	
Current sheet	10	40	
Plasma flux (tailward)			
Mass	1×10^{26}	5×10^{27}	amu s^{-1}
Number	6×10^{24}	3×10^{26}[e]	ions s^{-1}

[a]Parameters from *McComas et al.* [1986*a*].
[b]Parameters from *McComas et al.* [1987].
[c]Tailward flow speed nearly constant at all locations across tail.
[d]Calculated from the ratio of $(\mathbf{J} \times \mathbf{B})_X$ force to the mass density.
[e]Approximately 1% of 2–5 × 10^{28} s^{-1} total cometary efflux.

sheet cross tail current density of ~ 100 nA m^{-2}. This calculation neglected the unmeasured (and probably much smaller) term due to variations of the cross tail field component with distance down the tail. The current density within the G-Z current sheet is ~ 70 times greater than at Venus. This is attributable to a thinner current sheet structure and the factor of 2–3 times greater magnetic field strengths in the adjacent tail lobes at G-Z as displayed in Figure 3. The calculated X components of the $\mathbf{J} \times \mathbf{B}$ forces in the two current sheets are displayed in the second row of Table 1. These forces point tailward (negative) throughout the current sheets and act to accelerate the mass loaded material and to restraighten the highly kinked magnetotail field configurations. The reacceleration force at Comet G-Z (10^{-15} N m^{-3}) is about a factor of ~ 100 times greater than at Venus ($\sim 10^{-17}$ N m^{-3}).

The remainder of Table 1 displays the plasma properties of the two magnetotails inferred from stress balance considerations [*McComas et al.*, 1986*a*; *McComas et al.*, 1987]. Interestingly, the flow speeds (row 3) within the two tails at the nearly equivalent distances studied are both essentially independent of cross tail location. However, the absolute magnitudes of these velocities are quite different, the flow speed at Venus (~ -370 km s^{-1}) being ~ 15 times greater that at G-Z (~ -25 km s^{-1}). Row 4 displays typical values for the plasma accelerations within the two tail current sheets derived from the ratio of the $(\mathbf{J} \times \mathbf{B})_X$ forces to the inferred plasma mass densities. The plasma acceleration in the Venus current sheet (~ 6200 m s^{-2}) is ~ 110 times greater than at G-Z (~ 55 m s^{-2}) for the comparable tail regions studied. This difference is still large (~ 11 times greater) when the accelerations are rescaled into units of R_{ip} s^{-2}.

Since the tailward velocities are essentially independent of cross tail location at ~ -12 R_{ip}, this distance separates regions of tail formation upstream and restraightening of the magnetotail configuration (tail dissipation) downstream. Upstream, a velocity shear between the higher-speed plasma flows in the lobes and lower speed flows in the current sheet must exist in order to produce the draped tail configuration in the first place. Downstream, the plasma acceleration, caused by the sling-shot effect of the tailward $\mathbf{J} \times \mathbf{B}$ forces in the current sheet, must act to reaccelerate the mass loaded and slowed plasma and reduce the field line tension. Since the tailward plasma acceleration in the G-Z current sheet is ~ 110 times smaller than at Venus, the cometary tail might be expected to extend to much greater distances than Venus'. In addition, when the Venus tail configuration has dissipated, the plasma flow should be at approximately the solar wind speed, while dissipation of the narrow tail structure at G-Z probably occurs while the plasma is still flowing at the appreciably slowed magnetosheath speeds. A very broad region of sheath type field draping may therefore extend considerably further tailward of a comet than the narrow tail itself does. For example, Earth may have passed through some remnant field perturbation $\sim 2 \times 10^7$ km behind Comet Halley during its 1910 apparition (C. T. Russell et al., unpublished manuscript, 1986).

The next two rows of the table give the typical number densities in the current sheets (row 5) and lobes (row 6) of the G-Z and Venus magnetotails. The ratio between the current sheet and lobe densities are quite similar, being ~ 6 for G-Z and ~ 12 for Venus. On the other hand, the ratio of the densities in the two tails is very great, with the density at G-Z being $\sim 10^4$ times greater than the density at Venus.

In rows 7 and 8 of Table 1, the approximate inferred ion temperatures in the lobes and current sheets of the Venus and G-Z magnetotails are compared. In the Venus analysis, insufficient information was available to derive independent ion temperatures for the two regions. A single derived value of 9×10^7 K (for H_2O^+) therefore represents an intermediate temperature between somewhat higher lobe and somewhat lower current sheet values. Comparing this value with an average of the lobe and current sheet values at G-Z ($\sim 4 \times 10^5$ K) indicates that the ions are ~ 240 times hotter in the Venus tail than in the G-Z tail.

Ion temperatures in the two tails are indicative of the flow speeds in the upstream regions very near to the obstacles, where most of the heavy ions found in the tails were picked up. When a neutral atom or molecule is ionized it instantly is picked up by the plasma flow with initial parallel and perpendicular velocities which vectorially add to give minus the plasma flow velocity vector in the flowing plasma's frame. Eventually, the picked up ions pitch angle scatter into a spherical shell distribution in phase space, centered at the plasma rest frame velocity [e.g., *Winske et al*, 1985; *Omidi and Winske*, 1986]. Ultimately, particle scattering thickens this shelllike distribution into a filled in, more thermallike distribution.

The bottom two sections of Table 1 display the betas (rows 9 and 10) and total integrated tailward mass (row 11) and number (row 12) fluxes for the G-Z and Venus magnetotails. Beta is a measure of the relative importance of the particle and field pressures for the dynamics of a plasma. In the current sheets at both G-Z and Venus, beta is appreciably greater than 1, and the regions are both plasma pressure dominated. In the two lobes, on the other hand, the betas are quite different. The Venus tail lobes, much like Earth's, are low beta and dominated by the field. G-Z's lobes, however, have a beta slightly in excess of one and therefore are slightly plasma dominated.

The tailward mass fluxes and equivalent ion number fluxes for the two tails were derived by integrating the mass flux over the cross-sectional area of the tail. These fluxes are primarily transported down the tail current sheets, since the tailward flow speeds are relatively constant across the tails at the distances studied, while the current sheet densities are factors of ~ 12 and ~ 6 greater than in the lobes for G-Z and Venus, respectively. In the steady state, the total mass fluxes down the tails must provide a global measure of the mass loading which is associated with each tail. The total tail mass loading of the G-Z magnetotail ($\sim 5 \times 10^{27}$ amu s^{-1}) is ~ 50 times greater than that of the Venus magnetotail ($\sim 1 \times 10^{26}$ amu s^{-1}). While much greater than at Venus, the mass carried down the G-Z magnetotail is only $\sim 1\%$ of the total mass lost by the comet to the solar wind [*McComas et al*, 1987].

5. Discussion

In this study we have quantitatively compared and contrasted the (1) spatial scale sizes, (2) electromagnetic configurations and properties, and (3) consistent plasma properties of the Comet Giacobini-Zinner and Venus magnetotails. These two magnetotails form through the same physical process: magnetic field draping due to a velocity shear between stream lines which pass at varying distances from the planetary or cometary obstacle. Not surprisingly therefore these two magnetotails display qualitatively similar magnetic configurations.

Quantitatively, however, the electromagnetic and plasma properties in the two are quite dissimilar, indicating important differences in the ways that the two obstacles interact with the solar wind.

We contend that these similar tail configurations but quantitatively different tail properties are fundamentally attributable to two aspects of the solar wind interaction with unmagnetized but conductive and mass loading bodies. We believe that the magnetotails have similar magnetic configurations because the essential magnetotail forming magnetic field draping occurs in the near ionopause environs both when there is substantial upstream mass loading (such as at comets) and when there is not (such as at Venus). On the other hand, we believe that the numerous quantitative differences between the electromagnetic and plasma properties within the two tails are primarily attributable to significant differences in the conditions just upstream from the ionospheric obstacle resulting from very different mass loading from the extended versus gravitationally bound atmospheres. In this section we examine each of these two aspects of tail formation in turn.

5.1. *The Ionopause and Tail Similarities*

The claim that the very near environs to the ionopause are crucial for the formation of draped magnetotails, and therefore that similarities between the two magnetotails are driven by draping about these ionospheres, is verified independently by two aspects of our analysis. First, we have noted that the current sheet thicknesses at both G-Z and Venus are comparable to widths of the respective ionospheric obstacles presented to the solar wind. This indicates that the major slowing and mass loading which accounts for the formation of a well-defined, high-density, relatively cold, field-reversing current sheet probably occurs very near to the conductive ionopause.

Second, the small scale size of the G-Z magnetotail compared to the much larger region of interaction with the solar wind further shows the importance of the region very near to the ionopause for tail formation. The G-Z magnetotail occupies less than $\sim 0.1\%$ of the volume behind the cometary bow wave, and the flow within the magnetotail carries away only $\sim 1\%$ of the total cometary efflux. If draped magnetotails formed about mass loading obstacles rather than electrically conductive, ionospheric obstacles, then the magnetotail at G-Z might be expected to form over a larger region which encompassed a greater fraction of the total added cometary ions. While some field draping does occur about this broader region of mass loading, it might best be described as "magnetosheath" type draping which occurs so gradually and over such a large scale size that it cannot account for either the observed juxtaposition of two narrow and nearly antiparallel pointing tail lobes or the well-defined magnetotail boundary.

Three-dimensional MHD simulations of the solar wind interaction with G-Z [*Fedder et al.*, 1986], which simply model the ion source rate as a smoothly decreasing function with distance from the nucleus, generally exhibit a smooth variation in field rotation over a region which is appreciably wider than the observed magnetotail. These simulations, while excellent predictors of the more distant regions of the cometary-solar wind interaction, do not account for either the well-defined nature of the observed tail boundary, or the small size scale of the tail. The important physical difference between these simulations and the situation indicated by the in situ observations is that the simulations suffer from the use of grid point spacings of $\sim$few $\times 10^3$ km. Such a spatial resolution is clearly insufficient for resolving the strong gradients in plasma properties just upstream from the ionopause which play a crucial role in the actual tail formation process.

Because of the fundamental relation between the ionopause and magnetotail draping brought out in this study, ionopause radii provide a natural scale size for examining the properties of draped magnetotails. In light of this scaling, it was fortuitous for the purposes of this comparison that the only spacecraft traversal of a cometary magnetotail (i.e., ICE at G-Z) and the largest Venus tail data set (i.e., PVO) occurred at comparable numbers of ionopause radii back in the two magnetotails.

5.2. *Extended Mass Loading and Tail Differences*

In contrast to the similarities between the two tails, caused by the ionopauses at both bodies, the primary quantitative difference between the two draped magnetotails is attributable to differences in mass loading upstream from the two ionospheric obstacles. The bulk flow speed is ~ 15 times slower and picked up ion temperatures ~ 240 times colder in the analogous region of the G-Z magnetotail compared to that at Venus while tailward $\mathbf{J} \times \mathbf{B}$ forces, ion densities, downtail mass fluxes, and lobe betas are factors of ~ 100, 10^4, 50, and 20 times greater in the G-Z tail than in the Venus tail. These significant quantitative differences are directly related to the spatial extents of the respective atmospheres.

The extended mass loading region at G-Z causes the flow along stream lines which map into the tail to be factors of 10 times slower in the region just upstream from the ionopause compared to the far upstream solar wind. As a result, the flowing plasma spends more time in the region closest to the obstacle where the ion addition rates are highest. This leads to very high densities within the magnetotail current sheet of the comet compared to that at Venus. In addition, since the pick up temperature is proportional to the square of the perpendicular plasma velocity at the pick up location ($T = mv^2/3k$, where k is Boltzman's constant) the ion temperatures found in the G-Z tail are some hundreds of times lower than they would have been if the cometary ions (H_2O^+, etc.) had been picked up at the solar wind speed ($\sim 2 \times 10^8$ K). At Venus, on the other hand, tail ion temperatures in the high 10^7 K range indicate that pick up O^+ ions were primarily added to the flow in regions where the flow speed was still a substantial fraction of the solar wind speed, consistent with the lack of an extended mass loading region. Clearly, the effect of mass loading over an extended region upstream from an obstacle is to alter the properties of the plasma and imbedded field impinging on that obstacle; this alteration strongly modifies the properties within the magnetotail which forms behind it.

Since the flow which forms magnetotails at extended mass loading obstacles is slowed upstream from the tail formation region, the pick up speeds and therefore ion temperatures are much lower while the densities are much higher. In addition, since plasma flows at such obstacles are substantially slowed, a parcel of plasma spends appreciably more time in the region closest to the obstacle where ion addition rates are highest. This further slows the flow and acts as a positive feedback loop to drive very high densities and low flow speeds at such obstacles. This positive feedback process could explain the large gradients in near ionopause plasma properties needed for the formation of a well-defined magnetotail and magnetotail current sheet (ion tail) and might explain why small differences between the neutral outputs of different comets or

in the neutral output of a single comet can cause large differences in the lengths, column densities, and plasma flow speeds of visible ion tails. For example, there was a large difference in observed ion tail lengths between the long ion tail observed in the 1957 apparition of comet G-Z and the 1985 apparition with little or no visible ion tail. A positive mass loading–flow slowing feedback process, as suggested here, could allow a small decrease in neutral cometary efflux between the 1957 and 1985 apparitions to drive this large observed difference in the ion tail properties.

6. SUMMARY

The detailed comparison of the G-Z and Venus magnetotails has provided not only an excellent opportunity to extend our understanding of these two structures, but also has provided a unique opportunity to generalize our understanding of the tail formation process at unmagnetized but conductive and mass loading bodies. We find that draped magnetotails form from velocity shears in regions of strong gradients in plasma flow speeds and ion source rates, such as at the ionopauses of unmagnetized bodies. Therefore draped magnetotail structures scale as the impenetrable obstacle sizes where these strong density gradients exist (Figure 2). We further find that an extended mass loading region does not cause a larger tail structure to form, but rather serves to preslow the plasma flow upstream from the tail forming obstacle and thereby significantly alters the properties of the magnetotail which forms within it, as quantitatively compared for G-Z and Venus in Table 1. Finally, we suggest that the effects of mass loading in the near ionopause regions, where the flow is already most highly slowed and where the ion source rates are highest, should supply a positive feedback loop which can drive the local plasma densities very high and flow speeds very low, and thereby account for the large gradients in near ionopause plasma properties needed for draped magnetotail formation and explain the large observed differences in ion tails between various cometary apparitions.

Acknowledgments. We gratefully acknowledge valuable discussions of the Venus–solar wind interaction with J. L. Phillips. The research performed at the Jet Propulsion Laboratory of the California Institute of Technology was carried out under contract to NASA, while the work performed at UCLA was supported by NASA under contract NAS2-12383 and grant NAGW-717. Work done at Los Alamos National Laboratory was performed under the auspices of the United States Department of Energy with support from NASA under contract S-04039-D. Finally, we are indebted to both referees for their valuable comments and suggestions.

The Editor thanks J. A. Fedder and M. A. Saunders for their assistance in evaluating this paper.

REFERENCES

Alfvén, H., On the theory of comet tails, *Tellus*, *9*, 92, 1957.

Bame, S. J., et al., Comet Giacobini-Zinner: A plasma description, *Science*, *232*, 356, 1986.

Biermann, L., B. Brosowski, and H. U. Schmidt, The interaction of the solar wind with a comet, *Sol. Phys.*, *1*, 254, 1967.

Brace, L. H., R. F. Theis, H. G. Mayr, S. A. Curtis, and J. G. Luhmann, Holes in the nightside ionosphere of Venus, *J. Geophys. Res.*, *87*, 199, 1982.

Fedder, J. A., J. G. Lyon, and J. L. Giuliani, Jr., Numerical simulations of comets: Predictions for Comet Giacobini-Zinner, *Eos Trans. AGU*, *67*, 17, 1986.

Harwit, M., and F. Hoyle, Plasma dynamics in comets, 2, Influence of magnetic fields, *Astrophys. J.*, *135*, 875, 1962.

Ip, W.-H., and W. I. Axford, Theories of physical processes in cometary comae and tails, in *Comets*, edited by L. L. Wilkening, p. 588, University of Arizona Press, Tucson, 1982.

Marubashi, K., J. M. Grebowsky, H. A. Taylor, Jr., J. G. Luhmann, and A. Barnes, Ionosheath plasma flow in the wake of Venus and the formation of ionospheric holes, *J. Geophys. Res.*, *90*, 1385, 1985.

McComas, D. J., H. E. Spence, C. T. Russell, and M. A. Saunders, The average magnetic field draping and consistent plasma properties of the Venus magnetotail, *J. Geophys. Res.*, *91*, 7939, 1986*a*.

McComas, D. J., H. E. Spence, and C. T. Russell, The average configuration of the induced Venus magnetotail, in *Monograph on Magnetotail Physics*, Johns Hopkins University, Laurel, Md., 1986*b*.

McComas, D. J., J. T. Gosling, S. J. Bame, J. A. Slavin, E. J. Smith, and J. L. Steinberg, The Giacobini-Zinner magnetotail: Tail configuration and current sheet, *J. Geophys. Res.*, *92*, 1139, 1987.

Mendis, D. A., E. J. Smith, B. T. Tsurutani, J. A. Slavin, D. E. Jones, and G. L. Siscoe, Comet-solar wind interaction: Dynamical length scales and models, *Geophys. Res. Lett.*, *13*, 239, 1986.

Meyer-Vernet, N., P. Couturier, S. Hoang, C. Perche, J. L. Steinberg, J. Fainberg, and C. Meetre, Plasma diagnosis from thermal noise and limits on dust flux or mass in Comet P/Giacobini-Zinner, *Science*, *232*, 370, 1986.

Mihalov, J. D., and A. Barnes, Evidence for the acceleration of ionospheric O^+ in the magnetosheath of Venus, *Geophys. Res. Lett.*, *8*, 1277, 1981.

Omidi, N., and D. Winske, Simulation of the solar wind interaction with the outer regions of the coma, *Geophys. Res. Lett.*, *13*, 397, 1986.

Perez-de-Tejada, H., Viscous dissipation at the Venus ionopause, *J. Geophys. Res.*, *87*, 7405, 1982.

Russell, C. T., J. G. Luhmann, R. C. Elphic, and F. L. Scarf, The distant bow shock and magnetotail of Venus: Magnetic field and plasma wave observations, *Geophys. Res. Lett.*, *8*, 843, 1981.

Saunders, M. A., and C. T. Russell, Average dimension and magnetic structure of the distant Venus magnetotail, *J. Geophys. Res.*, *91*, 5589, 1986.

Scarf, F. L., F. V. Coroniti, C. F. Kennel, D. A. Gurnett, W.-H. Ip, and E. J. Smith, Plasma wave observations at Comet Giacobini-Zinner, *Science*, *232*, 377, 1986.

Siscoe, G. L., J. A. Slavin, E. J. Smith, B. T. Tsurutani, D. E. Jones, and D. A. Mendis, Statics and dynamics of Giacobini-Zinner magnetic tail, *Geophys. Res. Lett.*, *13*, 287, 1986.

Slavin, J. A., E. J. Smith, and D. S. Intriligator, A comparative study of distant magnetotail structure at Venus and Earth, *Geophys. Res. Lett.*, *11*, 1074, 1984.

Slavin, J. A., E. J. Smith, B. T. Tsurutani, G. L. Siscoe, D. E. Jones, and D. A. Mendis, Giacobini-Zinner magnetotail: ICE magnetic field observations, *Geophys. Res. Lett.*, *13*, 283, 1986*a*.

Slavin, J. A., B. A. Goldberg, E. J. Smith, D. J. McComas, S. J. Bame, M. A. Strauss, and H. Spinrad, The structure of a cometary Type I tail: Ground-based and ICE observations of P/Giacobini-Zinner, *Geophys. Res. Lett.*, *13*, 1085, 1986*b*.

Slavin, J. A., E. J. Smith, P. W. Daly, K. R. Flammer, G. Gloeckler, B. A. Goldberg, D. J. McComas, F. L. Scarf, and J. L. Steinberg, The P/Giacobini-Zinner magnetotail, in *The Proceedings of the 20th ESLAB Symposium*, European Space Agency, Noordwijk, The Netherlands, 1987.

Smith, E. J., B. T. Tsurutani, J. A. Slavin, D. E. Jones, G. L. Siscoe, and D. A. Mendis, ICE encounter with Giacobini-Zinner: Magnetic field observations, *Science*, *232*, 382, 1986.

Spreiter, J. R., and S. S. Stahara, Solar wind flow past Venus: Theory and comparisons, *J. Geophys. Res.*, *85*, 7715, 1980.

Winske, D., C. S. Wu, Y. Y. Li, Z. Z. Mou, and S. Y. Guo, Coupling of newborn ions into the solar wind by electromagnetic instabilities and their interaction with the bow shock, *J. Geophys. Res.*, *90*, 2713, 1985.

Zwickl, R. D., D. N. Baker, S. J. Bame, W. C. Feldman, S. A. Fuselier, W. F. Huebner, D. J. McComas, and D. T. Young, Three component plasma electron distribution in the intermediate ionized coma of Comet Giacobini-Zinner, *Geophys. Res. Lett.*, *13*, 401, 1986.

J. T. Gosling and D. J. McComas, Los Alamos National Laboratory, MS D438, Los Alamos, NM 87545.

C. T. Russell, Department of Earth and Space Sciences, University of California, Los Angeles.

J. A. Slavin, Jet Propulsion Laboratory, 4800 Oak Grove Drive, Pasadena, CA 91109.

(Received February 25, 1987;
revised May 18, 1987;
accepted June 4, 1987.)